International Journal of
Molecular Sciences

MDPI

Article

The Large GTPase Guanylate-Binding Protein-1 (GBP-1) Promotes Mitochondrial Fission in Glioblastoma

Ryan C. Kalb [1,†], Geoffrey O. Nyabuto [1,†], Michael P. Morran [2], Swagata Maity [1], Jacob S. Justinger [1], Andrea L. Nestor-Kalinoski [2] and Deborah J. Vestal [1,*]

[1] Department of Biological Sciences, University of Toledo, 2801 W. Bancroft St., Toledo, OH 43606, USA; ryankalb2@gmail.com (R.C.K.); nyabutogeoffrey@yahoo.com (G.O.N.); maityswagata94@gmail.com (S.M.); jacob.justinger@nemours.org (J.S.J.)
[2] Department of Surgery, University of Toledo, 3000 Arlington Ave., Toledo, OH 43614, USA; michael.morran@utoledo.edu (M.P.M.); andrea.kalinoski@utoledo.edu (A.L.N.-K.)
* Correspondence: deborah.vestal@utoledo.edu
† These authors contributed equally to this work.

Abstract: Glioblastomas (aka Glioblastoma multiformes (GBMs)) are the most deadly of the adult brain tumors. Even with aggressive treatment, the prognosis is extremely poor. The large GTPase Guanylate-Binding Protein-1 (GBP-1) contributes to the poor prognosis of GBM by promoting migration and invasion. GBP-1 is substantially localized to the cytosolic side of the outer membrane of mitochondria in GBM cells. Because mitochondrial dynamics, particularly mitochondrial fission, can drive cell migration and invasion, the potential interactions between GBP-1 and mitochondrial dynamin-related protein 1 (Drp1) were explored. Drp1 is the major driver of mitochondrial fission. While GBP-1 and Drp1 both had punctate distributions within the cytoplasm and localized to regions of the cytoplasmic side of the plasma membrane of GBM cells, the proteins were only molecularly co-localized at the mitochondria. Subcellular fractionation showed that the presence of elevated GBP-1 promoted the movement of Drp1 from the cytosol to the mitochondria. The migration of U251 cells treated with the Drp1 inhibitor, Mdivi-1, was less inhibited in the cells with elevated GBP-1. Elevated GBP-1 in GBM cells resulted in shorter and wider mitochondria, most likely from mitochondrial fission. Mitochondrial fission can drive several important cellular processes, including cell migration, invasion, and metastasis.

Keywords: Dynamin-like Proteins (DLPs); Epidermal Growth Factor Receptor (EGFR); glioblastoma multiforme (GBM); Guanylate-Binding Protein-1 (GBP-1); immunofluorescence; mitochondrial dynamin-related protein 1 (Drp1); Translocase of Outer Mitochondrial Membrane 40 (TOMM40)

Citation: Kalb, R.C.; Nyabuto, G.O.; Morran, M.P.; Maity, S.; Justinger, J.S.; Nestor-Kalinoski, A.L.; Vestal, D.J. The Large GTPase Guanylate-Binding Protein-1 (GBP-1) Promotes Mitochondrial Fission in Glioblastoma. *Int. J. Mol. Sci.* **2024**, *25*, 11236. https://doi.org/10.3390/ijms252011236

Academic Editors: Michele Caraglia and Raffaele Addeo

Received: 25 September 2024
Revised: 14 October 2024
Accepted: 16 October 2024
Published: 19 October 2024

1. Introduction

Epidermal Growth Factor Receptor (EGFR) signaling plays an important role in the prognosis of Glioblastoma multiformes (GBMs). Up to 60% of GBMs have either amplified wild-type EGFR or mutant EGFRvIII (amplified or not) driving their proliferation and/or invasion [1,2]. This would suggest that anti-EGFR therapy would be a good approach for treatment of GBMs, but unfortunately anti-EGFR treatments have not proven efficacious in GBMs. As a consequence, some attention has shifted to identifying critical proteins downstream of EGFR signaling to target. One such protein is the large cytokine-induced GTPase, Guanylate-Binding Protein-1 (GBP-1) [3–6].

GBP-1 is part of a large protein family that are members of the dynamin superfamily of GTPases [7–11]. GBPs differ from most GTPases by hydrolyzing GTP to both GDP and GMP, which influences whether the proteins are monomers, dimers, or polymers [12–24]. GBP-1 is the best studied of the GBP family [16,24,25]. While most commonly studied for their role in immune responses, the study of GBPs also focuses on their complicated role in cancer development and progression [26–28]. The anti-tumor activity of GBP-1

was first highlighted by the finding that cytokine-induced inhibition of angiogenic growth factor-induced proliferation of cultured human endothelial cells (HUVECs) resulted in the expression of GBP-1 [29,30]. Expression of GBP-1 in HUVECs inhibited their proliferation [29]. GBP-1 also inhibited the invasion and angiogenic ability of endothelial cells by inhibiting the expression of matrix metalloproteinase-1 (MMP-1) in vitro and decreasing angiogenesis in vivo [30]. Additional data on whether GBPs are protective or promote tumorigenesis are conflicting [9,31,32]. The data suggest that the roles of GBPs in cancers depend on such variables as cell type and immunological environment [33]. Data suggest that some of the effects of GBP expression may be the consequence of whether the tumor is in a primarily interferon-driven environment versus a growth factor-driven one.

GBP-1 expression is significantly increased in GBM tumors compared to normal controls [3,6]. A high expression of GBP-1 in GBMs was significantly correlated with shorter overall survival [5,6] and shorter prognosis-free survival [6]. In fact, GBP-1 is an independent risk factor of prognostic value for GBMs [6].

Knockdown (KD) of GBP-1 in U87 GBM cells forced to over express EGFR (U87-EGFR cells) resulted in reduced EGF induction of MMP-1- and EGF-driven invasion in vitro [3]. Forced expression of GBP-1 in A1207 cells promoted cell invasion that was then attenuated by siRNA KD of MMP-1, prompting the conclusion that GBP-1 is required for the EGF induction of MMP-1 [3]. Forced expression of GBP-1 in both SHG44 (SHG44-GBP-1) and U251 (U251-GBP-1) GBM cells caused a modest but statistically significant increase in cell migration and a more significant increase in cell invasion in vitro [3]. Neither forced expression of GBP-1 in A1207 cells or KD of GBP-1 in U178 cells altered cell proliferation in vitro [3]. Forced expression of GBP-1 in SHG44 or U251 cells also did not alter cell proliferation in vitro [6]. Interestingly, the KD of GBP-1 in SNB19 GBM cells resulted in significantly less tumor invasion than in cells with control shRNA after an intracranial xenograft [3]. Both SHG44-GBP-1 and U251-GBP-1 cells exhibited greater tumor growth and shortened survival in murine intracranial xenographs compared to controls [6]. Together, these data demonstrate that GBP-1 promotes cell migration and invasion but not proliferation in GBM cells in vitro and promotes tumor formation in vivo.

To further understand how EGFR and GBP-1 affect GBM cells, the role of the oncogenic mutant of EGFR (EGFRvIII) in promoting GBP-1 activities was examined. GBM xenografts were generated, separated into three groups based on EGFR expression, and analyzed for gene expression. One group had wild-type unamplified EGFR, the second group had wild-type but amplified EGFR, and the third group expressed EGFRvIII with or without amplification [5]. In addition, upregulated GBP-1 mRNA was correlated/associated with EGFRvIII expression in 20 GBM tumor samples [4]. The expression of GBP-1 was about two-fold greater in EGFRvIII xenographs than in xenographs with wild-type EGFR ± amplification [4]. The forced expression of EGFRvIII in U87 GBM (U87-EGFRvIII) cells significantly upregulated GBP-1 compared to control U87 cells [4]. Unlike with normal EGFR, U87-EGFRvIII promoted cell proliferation and KD of GBP-1 in U87-EGFRvIII cells significantly inhibited tumor growth in vitro [4]. EGFRvIII overexpression in U87 cells promoted tumor growth in subcutaneously inoculated mice compared to parental cells, and the KD of GBP-1 in these cells significantly inhibited tumor growth [4]. Elevated expression of GBP-1 promoted cell invasion in xenograft intracranial injections and resulted in much larger tumor volumes. This elevated growth and invasion resulted in a significant reduction in the percentage of survival [4]. Unlike wild-type EGFR, EGFRvIII not only promotes migration/invasion in vitro but promotes cell proliferation.

In an effort toward determining the mechanism(s) by which GBP-1 promotes cell migration/invasion, the intracellular localizations of GBP-1 in GBM cells were analyzed. Surprisingly, GBP-1 strongly localized to the mitochondria in GBM cells by both confocal microscopy and subcellular fractionation. Specifically, GBP-1 localized to the cytosolic side of the outer membrane of mitochondria. GBP-1 expression resulted in the relocation of the mitochondrial dynamin-related protein 1 (Drp1) to the mitochondria, where GBP-1 and Drp1 co-localize. Forced expression of GBP-1 results in shorter, wider mitochondria. This

was intriguing since mitochondrial dynamics are associated with regulation of migration and invasion [34]. Our study shows that GBP-1 localizes to the mitochondria in GBM cell lines and can play a role in regulating their mitochondrial behavior to promote the shortening of the mitochondria.

2. Results

2.1. EGF Treatment Does Not Induce GBP-1 in All Cultured GBM Cells

To determine the universality of GBP-1 induction by EGFR signaling, GBM cell lines were treated with EGF or IFN-γ and analyzed for the induction of GBP-1 (Figure 1A). IFN-γ was used to confirm that the cells were able to make GBP-1. Interestingly, only four of the cell lines expressed little or no GBP-1 before treatment (U251, SNB19, U87, and LN229). EGF treatment modestly induced GBP-1 in only two of these (U87 and SNB19). GBP-1 was constitutively expressed in SNB75, SNB295, and T98G cells. It was modestly induced in SNB295 cells. GBP-1 levels were reduced in T98G cells with EGF treatment but remained the same in SNB75 cells (Figure 1A). All cells responded to IFN-γ by inducing GBP-1 (Figure 1A). Previous studies indicated that the induction of GBP-1 by EGFR signaling promoted invasion by inducing the expression of MMP-1 [3]. Surprisingly, only SNB75 cells responded to EGF treatment by inducing MMP-1 (Figure 1B). MMP-1 was modestly expressed in SNB295 cells prior to treatment but expression was lost after EGF or IFN-γ treatment (Supplemental Figure S1). MMP-1 was not expressed in any of the cells after treatment with IFN-γ. These data (along with information presented in the introduction) suggested that the EGFR-mediated induction of MMP-1 expression via GBP-1 and its promotion of migration is most likely not the only mechanism to promote migration and invasion of GBM cells by GBP-1.

2.2. GBP-1 Localizes to the Mitochondria of GBM Cells

As a step toward narrowing the determination of GBP-1 functions, the intracellular localization of GBP-1 in SNB75 cells was analyzed by indirect immunofluorescence (IF) (Figure 1C). Surprisingly, GBP-1 localized to elongated, filamentous structures that suggested mitochondria (Figure 1C). Co-staining SNB75 cells for TOMM40 and cytochrome c identified these structures as mitochondria (Figure 1C). Note that while all three proteins localize to the mitochondria, their distribution at the mitochondria is not completely overlapping (Figure 1C overlay). This is consistent with the different known localizations of the proteins. TOMM40 localizes to the outer membrane of the mitochondria as a component of the Outer Mitochondrial Membrane Transporter (Translocon) [35]. Cytochrome c localizes to the mitochondrial intermembrane space, where it serves as an electron transporter in the electron transport chain [36].

To confirm that GBP-1 associates with mitochondria, SNB75 cells were subcellularly fractionated to isolate mitochondria (Figure 1D). As expected, TOMM40 localized to the mitochondria (M). A very small amount of TOMM40 could be found in the cytosolic fraction (C), which could be accounted for by the fact that the gene for TOMM40 is nuclear (National Library of Medicine, Gene ID: 10452. Updated 26 January 2024). GBP-1 localized to both the mitochondria and the cytosol (Figure 1D). The intracellular localization of GBP-1 by indirect IF suggests that most of the GBP-1 is associated with mitochondria in SNB75 cells but the subcellular fractionation suggests that most of the GBP-1 is associated with the cytoplasm. GBP-1 is a lipid-anchored protein that can form polymers and can come on and off cellular membranes using the farnesyl lipid on its C-terminus [37–39]. The observation that after subcellular fractionation most of the GBP-1 localized to the cytosol suggests a loose association of GBP-1 with the mitochondria that can be easily dissociated.

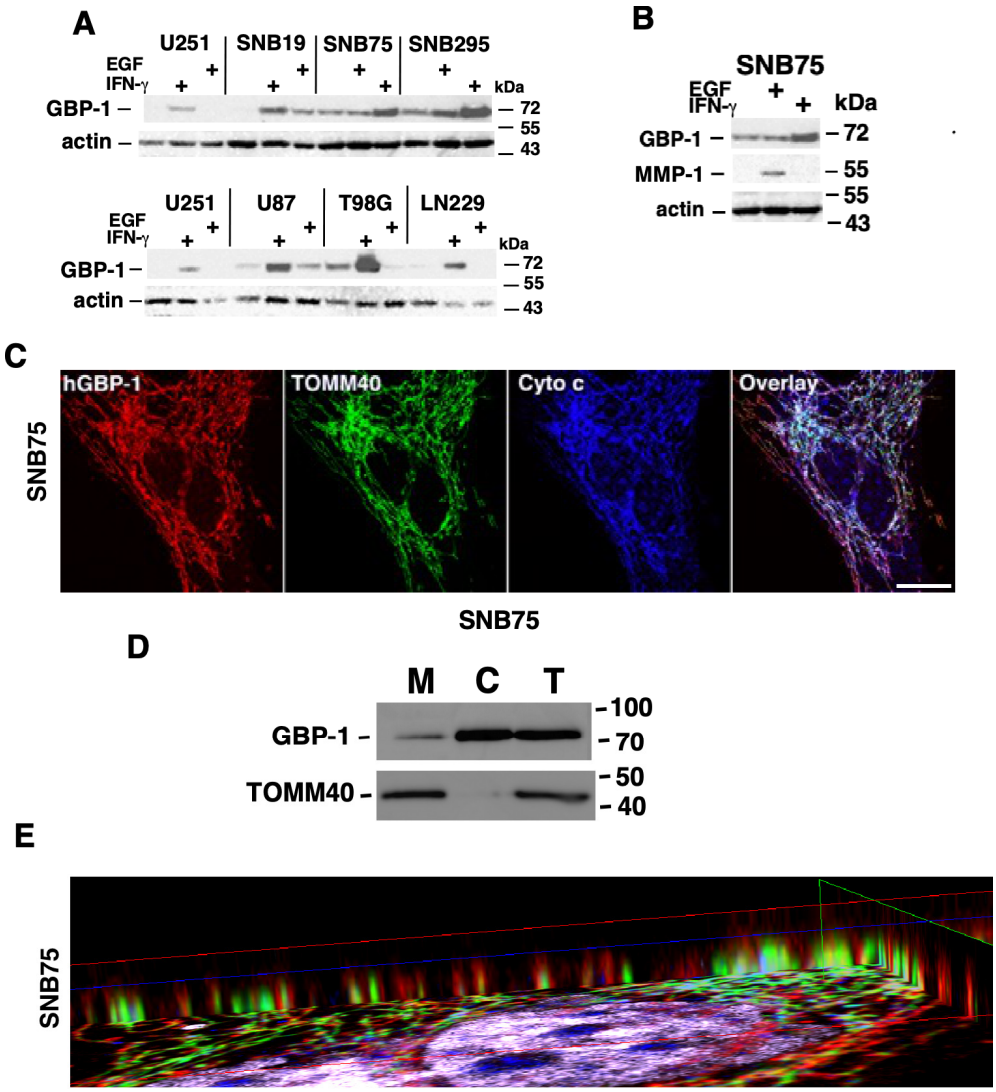

Figure 1. GBP-1 localizes to mitochondria in SNB 75 glioblastoma cells by indirect immunofluorescence. (**A**) GBM cell lines were plated overnight and then serum-starved for 24 h. Cells were either left untreated or treated with 50 ng/mL hEGF or 500 U/mL of hIFN-γ for 24 h. Cell lysates (20 μg) were separated by 8% SDS-PAGE, followed by western blot (WB) for GBP-1 and actin. (**B**) WB of SNB75 is shown with a lane for MMP-1 expression. (**C**) SNB75 cells were analyzed by triple-label IF to determine the intracellular location of GBP-1. After incubating with antibodies against GBP-1, TOMM40, and cytochrome c, cells were incubated with appropriate highly cross-adsorbed secondaries, mounted, and images were capture by confocal microscopy at 0.2 μm optical sections. Size bars = 25 μm. (**D**) SNB75 cells were fractionated into mitochondrial (M) and cytosolic (C) fractions and analyzed for GBP-1 and TOMM40 by WB. Total cell lysates (T) were also provided. (**E**) SNB75 cells were analyzed by multiphoton confocal microscopy. The image series from one z-stack is shown in Figure 1C. SNB75 images were compiled and analyzed by 3D reconstruction. Visualization of the image from the side shows that the TOMM40 signal (green) for the outer mitochondrial membrane is surrounded by the signal for GBP-1. This indicates that GBP-1 is on the outside of the outer mitochondrial membrane.

2.3. GBP-1 Localizes to the Outer Membrane of Mitochondria

To get a clearer idea of where GBP-1 resides on mitochondria, images of SNB75 cells captured in Figure 1C were compiled and analyzed by 3D reconstruction. Visualization of the image from the side shows that the TOMM40 signal (green) for the outer mitochondrial membrane is surrounded by GBP-1 (red) (Figure 1E). This indicates that GBP-1 is

on the cytosolic side of the outer mitochondrial membrane, which would be consistent with it being a lipid-anchored protein relatively loosely associated with the cytosolic side of mitochondria.

To confirm that the localization of GBP-1 to GBM mitochondria was not unique to SNB75 cells, U251 cells expressing myc-tagged GBP-1 were generated (Figure 2A). The cells will be designated U251+/-GBP-1 in the future. Triple-label IF again demonstrated that GBP-1 localizes to the mitochondria (Figure 2B). Interestingly, the morphologies of the mitochondria were very different between the two cell lines. The mitochondria of SNB75 cells were much more elongated and tubular than those of the U251 cells, despite both cell lines expressing GBP-1 that localized to the mitochondria. The far-right panel of this figure shows an enlargement of the area within the square in the cytochrome c panel. Consistent with the staining of SNB75, while all three proteins are found at the mitochondria, they are in slightly different locations. Again, to get a clearer idea of where GBP-1 resides on mitochondria, images of U251+GBP-1 cells were compiled and analyzed by 3D reconstruction. While the morphology of the mitochondria in these cells was less tubular than that in the SNB 75 cells, visualization of the image from the side again shows that the TOMM40 signal (green) for the outer mitochondrial membrane is surrounded by GBP-1 (red) (Figure 2C), again indicating that GBP-1 localizes to the cytosolic side of the outer membrane of mitochondria.

2.4. GBP-1 Did Not Promote Migration in U251 Cells, as Measured by Scratch Assays

To determine whether our U251 cells responded to GBP-1 by enhancing migration, U251 and U251+GBP-1 cells were analyzed for migration by scratch assay (Supplementary Figure S2). U251 cells closed their wounds 4 to 6 h faster than U251+GBP-1 cells (Supplementary Figure S2A). The wounds of U251 cells closed within 14 h after wounding and the U251+GBP-1 cells closed their wounds in about 20 h. At least one experiment using the U251+GBP-1 (D7) cell line also showed that they closed their wounds at 20 h (Supplementary Figure S2A). Closer examination of the wound closing curves shows that the presence of GBP-1 results in a flatter curve for the first 4 h after wounding than observed in the absence of GBP-1 (delineated by the box) (Supplementary Figure S2A). This suggests about a 4-hour lag time before starting to increase the speed of migration after wounding. This 4 hour "lag" was also observed for the U251+GBP-1 (D7) cells (Supplementary Figure S2A). Representative images of wound closures are shown (Supplementary Figure S2B). To determine the rate of wound closure, the slope of the graph of percent wound closure was determined from the closure data from 4 h to 14 h, chosen because of the "delay" in closure within the first 4 h and because the wound was closed for U251 cells by 14 h (Supplementary Figure S2C). The rate of wound closure was greater for U251 cells without the addition of exogenous GBP-1 (Supplementary Figure S2C).

To further determine how GBP-1 may alter the migration (as measured by wound closure after wounding), the rates of wound closure were determined for each of the 2-hour time increments post-wounding (Supplementary Figure S3A). As suggested by the wound closure curves (Supplementary Figure S2B), the rate of closure for U251 cells was faster from zero to 6 h than the U251+GBP-1 cells. Between 6 and 14 h, the rates of closure were more comparable. The changes of rates of closure over time are visualized graphically first for just the U251 and U251+GBP-1 (D4) cells and then for all three cell lines (Supplementary Figure S3B,C). It is unclear why our U251 cells did not migrate faster in the presence of GBP-1.

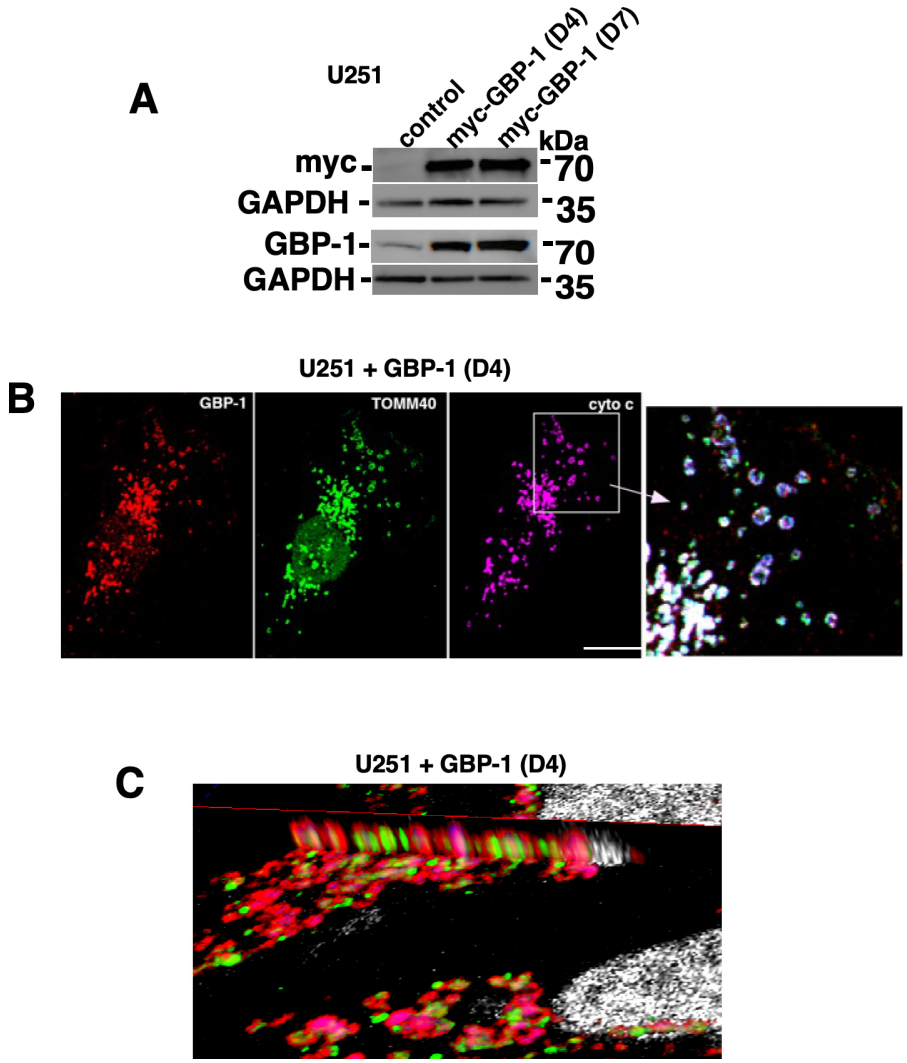

Figure 2. GBP-1 localizes to mitochondria in U251 cells. (**A**) U251 cells were generated to express myc-tagged GBP-1. Control cells (empty vector) and two pools of cells expressing myc-tagged GBP-1 were analyzed by WB for GBP-1 expression. (**B**) U251+GBP-1 (D4) cells were analyzed by triple-label IF for the localization of GBP-1 using antibodies against myc, TOMM40, and cytochrome c. The panel on the far right shows the overlay of the region of the photomicrograph designated by the box in the cytochrome c panel. Size bar = 20 μm. (**C**) U251+GBP-1 cells were analyzed by multiphoton confocal microscopy for the expression of TOMM40 and GBP-1. The images were compiled and analyzed by 3D reconstruction. Visualization of the image from the side suggests that the TOMM40 signal (green) for the outer mitochondrial membrane is surrounded by GBP-1 (red). This suggests that GBP-1 is on the outside of the outer mitochondrial membrane.

2.5. GBP-1 Can Promote Movement of Dynamin-Related Protein 1 (Drp1) to the Mitochondria

Cancer cell migration/invasion can be promoted by mitochondrial fission [40,41]. Mitochondrial fission is facilitated by the activation of the normally cytosolic Drp1 and its subsequent translocation to the outer membrane of the mitochondria, where it drives mitochondrial fission [34,40]. To determine whether GBP-1 promotes the movement of Drp1 to mitochondria, subcellular fractionation of U251 cells ± GBP-1 was used to determine the cellular location of Drp1. Drp1 is predominately in the mitochondrial fraction (M) in cells with empty vector but more Drp1 moves from the cytosol (C) to the mitochondria (M) in the presence of elevated GBP-1 (Figure 3A). In contrast, subcellular fractionation of SNB75 cells showed very little Drp1 associated with the mitochondria (M) (Figure 3B). The observation of little Drp1 associated with the mitochondria of SNB75 cells is consistent

with the long, tubular mitochondria found in these cells (Figure 1). U251 cells had much smaller mitochondria, suggesting mitochondrial fission was occurring even in the absence of exogenous GBP-1 (Figure 2).

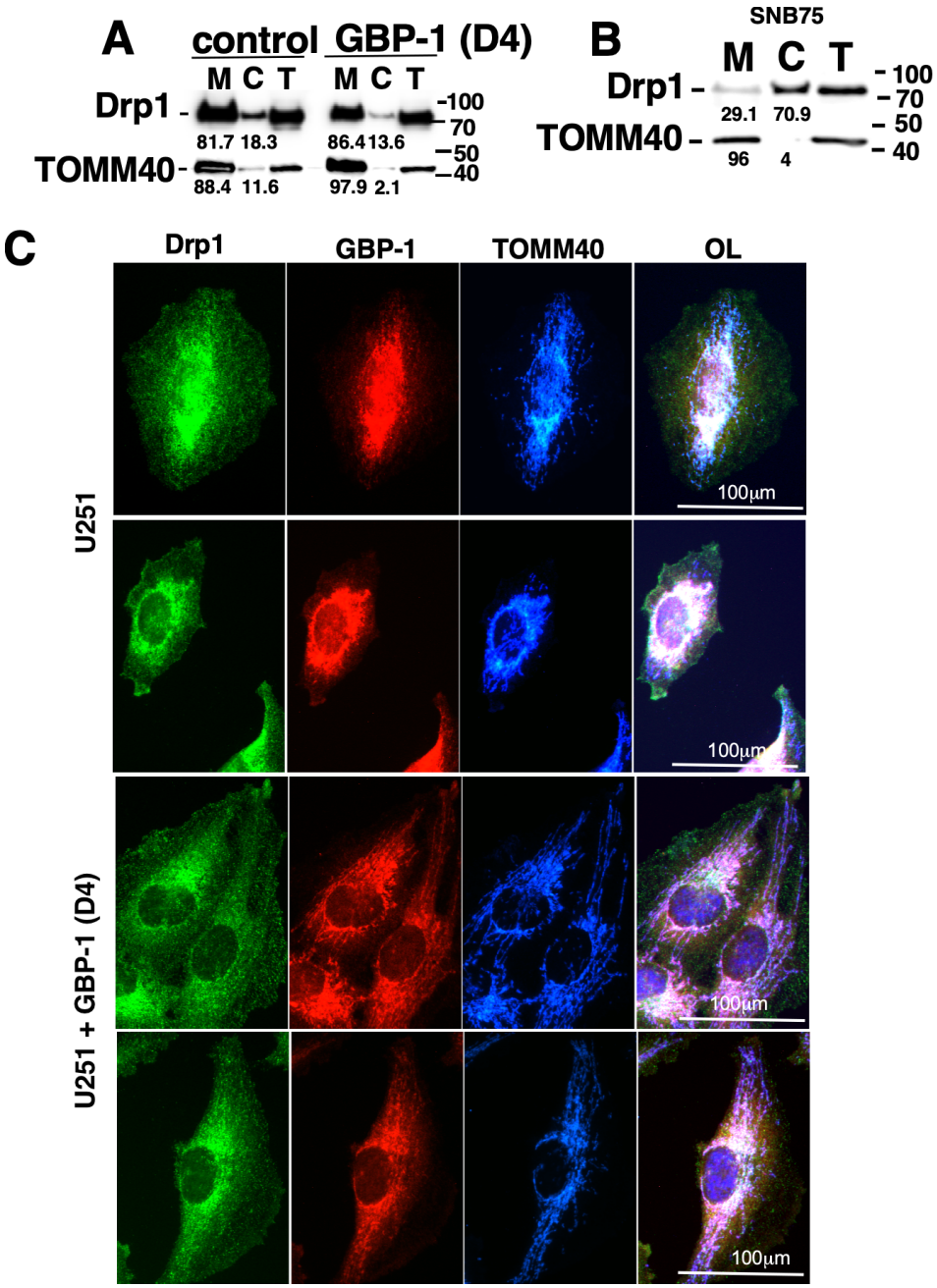

Figure 3. GBP-1 induces the translocation of Drp1 to the mitochondria. (**A**) Control (empty vector) and myc GBP-1-expressing U251 cells (D4) were fractionated into mitochondrial (M) and cytosolic fractions (C) and analyzed for Drp1 and TOMM40 by WB. Total cell lysates (T) are also provided. (**B**) SNB75 cells were fractionated into mitochondrial (M) and cytosolic fractions (C) and analyzed for Drp1 and TOMM40 by WB. The numbers under the blots are the percentage of the protein in each fraction. (**C**) Control U251 and U251+GBP-1 (D4) cells were plated on coverslips ON and then analyzed for the expressions of GBP-1, Drp1, and TOMM40 by indirect IF. Two representative examples of each cell type are shown.

To further analyze the intracellular location of Drp1, control U251 or U251+GBP-1 (D4) were analyzed by IF (Figure 3C). In the presence or absence of GBP-1, Drp1 distribution was punctate throughout the cytoplasm with some concentration around the nucleus. In

the absence of exogenous GBP-1, there is little GBP-1, so the intensity of the images were enhanced to see its localization. While some localization of GBP-1 with mitochondrial TOMM40 is observed, this co-localization is much more visible in the cells with exogenous GBP-1. Some of the Drp1 appears localized to mitochondria in the presence or absence of GBP-1. However, the mitochondrial staining was more spread out throughout the cells in the presence of GBP-1 and close examination suggested association with Drp1 along the mitochondrial tracks. This is consistent with the subcellular fraction (Figure 3A).

2.6. GBP-1 Makes U251 Cells Less Sensitive to Inhibition of Drp1

To determine whether the migration of U251 cells is sensitive to Drp1, U251 and U251+GBP- 1 (D4) cells were analyzed for changes in wound closure in the presence of different concentrations of the Drp1 inhibitor, Mdivi-1 (Supplementary Figure S4). Inhibition of migration of U251 cells (Supplementary Figure S4A) or U251+GBP-1 cells (Supplementary Figure S4B) by Mdivi-1 was dose dependent. The rates of wound closure at the different concentrations of Mdivi-1 were compared (Supplementary Figure S4C). As described previously, the rate of wound closure from 4 to 14 h post-wounding was significantly faster for U251 compared to U251+GBP-1 (D4) cells (Supplementary Figure S4A,B). While the rate of wound closure for both U251 and U251+GBP-1 cells was inhibited by Mdivi-1, the U251+GBP-1 (D4) showed a smaller decline than the U251 cells (Supplementary Figure S4C). As stated earlier, the rate of wound closure for untreated U251 cells was significantly shorter than for U251+GBP-1 cells (Supplementary Figures S2C and S4C). While the wound closure rates of both U251 and U251+GBP-1 cells were shortened by treatment with either 5 or 20 μM of Mdivi-1, the cells without exogenous GBP-1 were more sensitive to Mdivi-1 treatment (Supplementary Figure S4C). There was no longer a difference in the rate of wound closure between the two cell lines after treatment with either 5 μM or 20 μM drug. The data for 50 μM Mdivi-1 were not included because at this concentration there was evidence of cell toxicity (Supplementary Figure S5) (note the pycnotic nuclei). Consistent with the long tubular mitochondria of SNB 75 cells, little of the Drp1 localized to mitochondria (Figure 3C) and the cells closed their wounds more slowly and exhibited less sensitivity to Mdivi-1 (Supplementary Figure S4D).

2.7. Drp1 and GBP-1 Are Together at Mitochondria

To determine whether Drp1 localizes with GBP-1, U251+GBP-1 (D4) cells were analyzed by triple-label IF (Figure 4). Drp-1 localized throughout the cytoplasm in a punctate distribution but with concentrations at the inner plasma membrane (denoted by white arrowheads) and within cytosolic regions closer to the nucleus (Figure 4A). As observed previously, GBP-1 has a punctate distribution within the cytoplasm and at the inner plasma membrane (white arrowheads) (Figure 4B). However, much of the GBP-1 was associated with mitochondria (Figure 4B; green arrowhead designates GBP-1 associated with mitochondria in 4C). Close examination showed that the staining of larger structures for GBP-1 lines up with the mitochondrial staining for TOMM40 (Figure 4C; green arrowheads show mitochondria co-localizing with GBP-1). The mitochondria visualized by TOMM40 are larger and closer to the nucleus, with smaller mitochondria closer to the plasma membrane. Overlays were generated comparing only two of the proteins at a time for easier visualization. Comparing GBP-1 and Drp1 localization again shows that they both have punctate distributions within the cytoplasm and concentrate at the inner plasma membrane (Figure 4D). Amplification of the region shown in the box in 4D shows that while both Drp1 and GBP-1 went to the inner plasma membrane, they exhibit little or no co-localization (as evidenced by the yellow color; white arrowhead) (Figure 4D1). Neither did the individual puncta of the proteins in the cytoplasm co-localize (Figure 4D1; green arrowhead). "Co-localization" of the two proteins only occurred at mitochondria (Figure 4D,D1,E,E1,F,F1,F2).

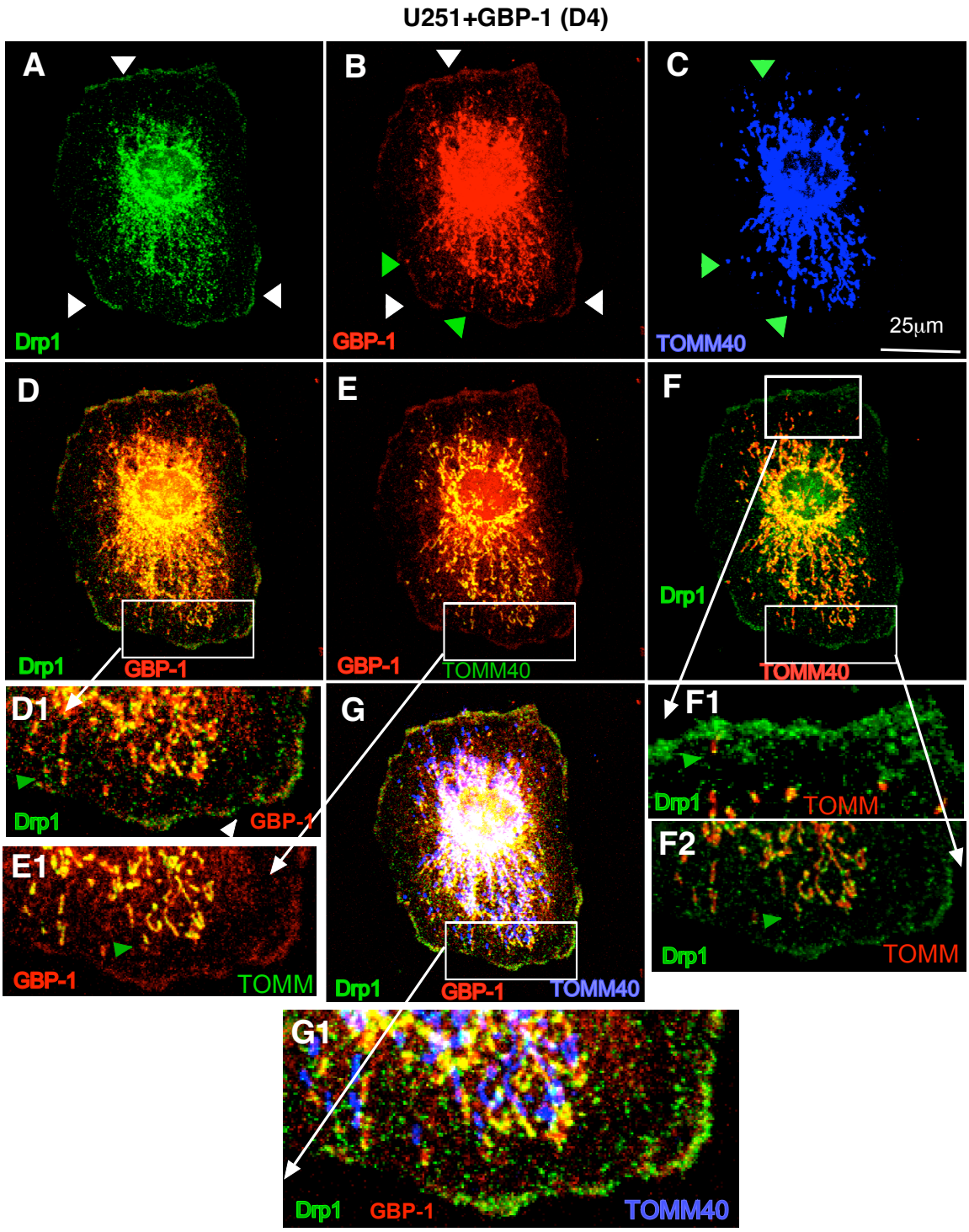

Figure 4. Drp1 colocalizes with GBP-1 at GBM mitochondria. U251 cells expressing myc GBP-1 (D4) were analyzed for the intracellular location of Drp1 (**A**), GBP-1 (**B**), and TOMM40 (**C**) by triple-label IF. Images were captured at 0.2 μm z-sections. (**D**) The images of Drp1 and GBP-1 staining are overlayed. The white box delineates the region amplified in (**D1**). (**E**) The images of GBP-1 and TOMM40 are overlayed and the white box delineates the region amplified in (**E1**). (**F**) The images of Drp1 and TOMM40 are overlayed and the white boxes delineate regions amplified in (**F1**,**F2**). (**G**) The overlay of Drp1, GBP-1 and TOMM40 is shown. The white box delineates the region amplified in (**G1**).

While both GBP-1 and Drp1 localized to the mitochondria, resulting in a yellow region suggesting "co-localization", close examination of the staining patterns of the two

proteins on mitochondria differed (Figure 4 all panels). GBP-1 staining covered more of the outer membrane of the mitochondria, as localized by TOMM40 (Figure 4E,E1,G,G1). Drp1 staining remains more punctate, even at the mitochondria (Figure 4E1,F,F1,F2,G,G1). It is often found at the terminus of mitochondria. This may reflect the retention of Drp1 at the severed mitochondria after fission. The localization of the mitochondria varied as fission proceeded. Drp1 localization with mitochondria could be observed at the lamellapodia in some cells (Supplementary Figure S6).

2.8. GBP-1 Results in Shorter, Wider Mitochondria

Mitochondrial fission is closely correlated with increased cell migration, invasion, lamellipodia formation, and turnover of focal adhesions [34,40,42]. The mitochondria in U251+GBP-1 cells (D4) were much less filamentous compared to those in the SNB75 cells (Figure 1C versus Figure 2B). To determine if GBP-1 alters mitochondrial dynamics in GBM cells, vector control U251 and U251+GBP-1 cells were stained for TOMM40 and the length and width of individual mitochondrion were measured (Figure 5). Representative figures of the mitochondria are shown (Figure 5A). GBP-1 resulted in mitochondria that were both shorter and wider than those in vector control cells (Figure 5B,C). Their elongation index, calculated from the length divided by the width of individual mitochondria, was also reduced. (Figure 5D). Together, these data indicate that GBP-1 results in shorter mitochondria, most likely by promoting fission.

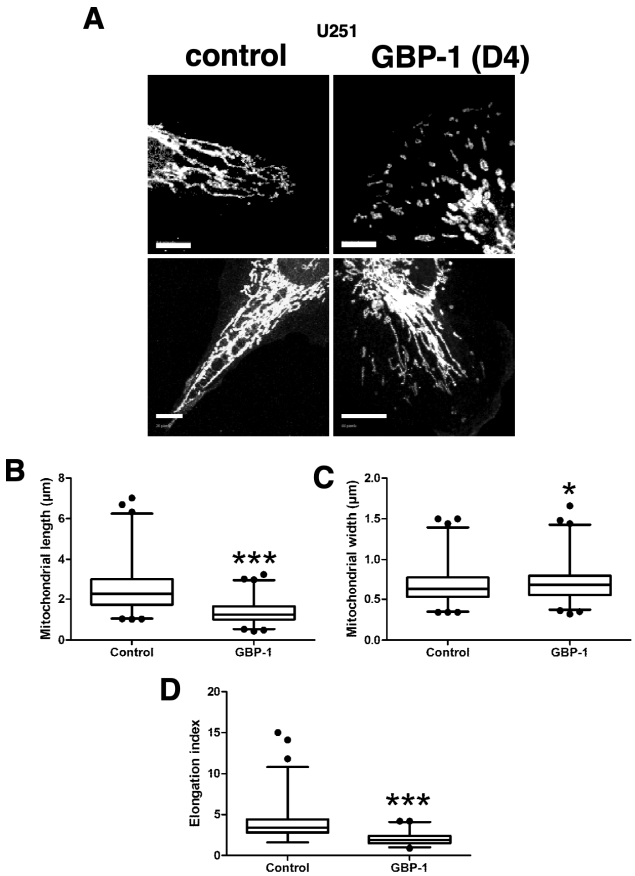

Figure 5. GBP-1 shortens glioblastoma cell mitochondria. U251 cells with (GBP-1) or without (control) myc-epitope-tagged GBP-1 were stained for TOMM40 and analyzed by confocal microscopy at 0.2 μm optical sections. (**A**) Representative examples of mitochondrial morphology are presented. Size bar = 10 μm. (**B**) The lengths of individual mitochondria were measured as described in Methods. (**C**) The width of individual mitochondria was measured as described. (**D**) The elongation index of individual mitochondria was calculated by dividing the length by the width. (n = 2; * = $p < 0.05$; *** = $p < 0.001$).

3. Discussion

The data from several studies of GBMs demonstrate a correlation of GBP-1 with poor prognosis [3,6]. Both overall and progression-free survival of patients with GBM were significantly less with higher expression of GBP-1 [5,6]. GBP-1 expression may be more elevated in GBM with EGFRvIII mutations than in tumors with a wild-type level or amplification of EGFR [5]. Whether GBP-1 promotes GBM progression by promoting cell migration and/or invasion was analyzed in vitro via Boyden chamber using either U251 or SHG44 GBM cells over-expressing GBP-1 [6]. The increase in migration observed was modest but the increase in invasion was 2–3-fold [6]. Even though the migration increase was modest, multiple genes associated with migration and invasion were increased, such as MMP-9, Twist, and Snail [6]. Intracranial injection of either U251 or SHG44 cells over-expressing GBP-1 resulted in larger tumors and significantly shorter survival times [6]. Conversely, the knockdown of GBP-1 in SNB19 cells with intracranial injection resulted in smaller tumors and fewer invasive cells [3]. In addition, the forced expression of GBP-1 in SHG44 or U251 cells promoted resistance to TMZ but not radiotherapy in vitro [3].

Our study demonstrates that GBP-1 localizes to GBM mitochondria (Figures 1–3). However, our data suggest that GBP-1 at the mitochondria is not always sufficient to promote mitochondrial fission (Figures 1–3). GBP-1 localizes to mitochondria in both U251 and SNB75 GBM cells, but only U251 cells are responsive to Drp1, and GBP-1 can further promote movement of Drp1 to the mitochondria (Figure 3) and act to modulate mitochondria activity. Consistent with this, elevated GBP-1 attenuated the inhibition of U251 cell migration after treatment with the Drp1 inhibitor, Mdivi-1 (Supplementary Figure S4). Fully understanding how GBP-1 enhances mitochondrial fission will still require more investigation. However, there are some properties of GBP-1 that can provide us with potential avenues for investigation. As a member of the dynamin super family, GBP-1 interacts with lipids, forms oligomers, and modifies membranes [13,28,38]. It also modulates both actin [39] and tubulin activity [40,42], both of which are important in mitochondrial fission [43–45]. However, it seems that the earlier steps of mitochondrial fission must occur before GBP-1 can promote further fission.

Both GBPs and Drp1 are GTPases that are members of the Dynamin Superfamily of Proteins (DSPs) [46]. These proteins can be subdivided into subfamilies with different properties and functions but there are some common properties of members of the DSPs [38,46–49]. One such common feature is the ability to alter membranes in a GTPase-dependent manner. Family members have a large GTPase domain and differ from many of the GTPases, such as members of the Ras superfamily of GTPases, by exhibiting oligomerization-dependent GTPase activity and a low affinity for GTP and GDP, and many exhibit binding to cellular membranes (reviewed in [13,38,41,45,47,50]). Drp1 and GBP-1 are found in two different subfamilies of DSPs [48,49]. Members of the dynamin family have low affinity for both GTP and GDP. Under normal cellular conditions, the proteins would be expected to be GTP bound. Unlike members of the Ras family of GTPases, members of the DSPs oligomerize, a process that stimulates GTPase activity. This oligomerization-dependent activity of the GTPase is usually preceded by membrane binding. The functions of DSPs include vesicle scission, organelle division and fusion, cytokinesis, and antiviral activity. It remains unclear how these two dynamin superfamily members, with membrane-binding and -altering activities, function together to promote mitochondrial fission.

Mitochondrial dynamics and their disruption play important roles in health and disease; one such disease being cancer [51–53]. Mitochondrial morphology and cellular location are important in determining cellular activities [52]. One such activity that influences mitochondria morphology and cellular location is mitochondrial fission. Mitochondrial fission is important because it generates smaller mitochondria that can be moved by the cytoskeleton to the leading edge of migrating/invading cells where energy is required [54]. Determination of mitochondrial shape and location are governed by complex processes, with many of these that promote mitochondrial fission working through Drp1 [40,55]. In addition to promoting mitochondrial fission, Drp1 may also play a role in lamellipodia

formation [56]. As a consequence of enhanced mitochondrial fission, cancer cells exhibit enhanced migration/invasion [34,35,57].

While significant progress has been made in understanding the mechanisms behind mitochondrial fission, there is much that is not yet clear (reviewed in [13,38,45–49,58]). One current model of mitochondrial fission can be divided into three steps. The first step involves the actin network of the ER beginning the constriction of mitochondria. This precedes the recruitment of Drp1 to the mitochondria. Drp1, the primary driver of mitochondrial fission, is primarily a cytosolic protein that relocates to the mitochondria when activated [58,59]. When activated by phosphorylation, Drp1 moves to the mitochondria, where it interacts with specific receptors on the outside of the outer membrane [34]. These activated Drp1 molecules are recruited to the pre-constricted regions of the mitochondria where GTP hydrolysis drives further constriction of the mitochondria. Drp1, however, cannot drive the process to the point of fission. The final steps for fission require the recruitment of Dynamin 1 (Dyn2) to the Drp1 already constricted regions. Much remains unclear about the steps involved, the co-factors required, and the cytoplasmic environment required for mitochondrial fission. The observation that GBP-1 can augment the fission process is intriguing. However, more experimentation is needed to determine how GBP-1 contributes to promoting fission.

4. Materials and Methods

4.1. Cells and Cell Culture

U251, U87, T98G, and LN229 glioblastoma cells were obtained from American Type Culture Collection (ATCC) and SNB19, SNB75, and SNB295 glioblastoma cells were the gift of William Maltese (University of Toledo). All were maintained in complete DMEM (Mediatech, Manassas, VA, USA) with 4.5g/L glucose which was supplemented with 10% fetal bovine serum (FBS; Atlanta Biologicals, Lawrenceville, GA, USA), 2mM L-glutamine (Mediatech, Manassas, VA, USA), and 50 µg/mL penicillin/streptomycin (Mediatech, Manassas, VA, USA). Stable cell lines containing control vector pIRES-hygro2 and high-expressing hGBP-1 c-myc-hGBP1-pIRES-hygro2 were maintained in complete DMEM with the addition of hygromycin (50 µg/mL) (Research Products International, Mount Prospect, IL, USA). All cells were cultured at 37 °C and five percent carbon dioxide. Cells were suspended by treatment with 0.05% trypsin/0.53 mM EDTA (Mediatech, Manassas, VA, USA). Cells were regularly checked for mycoplasma, which will induce interferons and alter the GBP-1 expression in "untreated" cells.

4.2. PAGE Gels and Western Blot (WB)

Cells at 80–85 percent confluence were lysed in RIPA buffer (50 mM Tris pH 7.5, 150 mM NaCl, 1% NP40, 0.5% sodium deoxycholate, and 0.1% SDS) containing 1 mM phenylmethylsulfonyl fluoride and one percent protease cocktail (Sigma Aldrich, St. Louis, MO, USA. Cell lysates (20 µg) were size fractionized by 8% polyacrylamide SDS-PAGE gels and transferred onto Immobilon-P membranes for 2 h at 100 volts in 1× transfer buffer (25 mM Tris, 0.192 M Glycine, 20% methanol) for WB analysis as previously described [36]. The membrane was blocked in blocking buffer (TBST (250 mM Tris, pH 8, 5 M NaCl, and 0.3% Tween-20) plus 5% nonfat dry milk) for 1 h at room temperature or overnight at 4 °C. After transfer, membranes received a primary antibody in blocking buffer for 1.5 h. The primary antibodies were rat anti-hGBP-1 (1b1) (Santa Cruz Biotechnology (SCBT), Dallas, TX, USA, 1:10,000); mouse anti-MMP1 Mab 901 (R&D Systems 1:750); rabbit anti-actin (Sigma 1:1000), rabbit anti-Translocase of Outer Mitochondrial Membrane 40 (TOMM40; (1:1500)), mouse anti-myc (1:2000), and mouse anti-Drp1 (1:100, SCBT, Dallas, TX, USA, sc-101270). Membranes received a secondary antibody diluted in blocking buffer for at least 1 h. The hrp-conjugated secondary antibodies were goat anti-rabbit IgG (1:1000; Invitrogen, Carlsbad, CA, USA), goat anti-rat IgG (1:1500; Rockland, Pottstown, PA, USA), and goat anti-mouse IgG (1:1000; Invitrogen). Antibodies were detected using Super Signal West Pico Chemiluminescent Substrate (Thermo, Carsbad, CA, USA), following the manufacturer's

instructions. At least 2 independent experiments were performed for each of the WBs. A representative figure is shown.

4.3. Immunofluorescence and Microscopy

Cells (50,000) were plated per cover slip in a 6-well dish and incubated for 24 h in complete DMEM (Mediatech, Manassas, VA, USA),). Cells were fixed with 4% paraformaldehyde (PFA) for 20 min and washed in phosphate buffer saline (PBS; 138 mM NaCl, 2.6 mM KCl, 5.4 mM Na2HPO4, 1.8 mM KH2PO4, pH 7.4). An antigen retrieval step was used only with primary anti-GBP-1 antibody 1b1 or any combination of antisera that contained 1b1. Cover slips were placed in antigen retrieval buffer (10 mM TRIS, 1.3 mM EDTA, 1L H_2O, pH 9) and submerged in a hot water bath at 95 °C for 10 min. Cells were then permeabilized with 0.1% Triton X-100 in PBS for 10 min and blocked with antibody dilution buffer (10% PBS, 0.05% Tween-20, 6% BSA, 5% Glycine) with 10% non-immune horse serum for 2 h. Cells were incubated with primary antibodies overnight at 4°, followed by PBS washes and the addition of secondary antibodies for 1 h at room temperature. Antibodies against TOMM40 (1:100; Proteintech, Rosemont, IL, USA (18409-1-AP)) and Cytochrome c (1:50; Abcam, Cambridge, UK) were used for mitochondrial staining. Anti-GBP-1 (1b1) (1:25; Calbiochem (Sigma, St. Louis, MO, USA) or SCBT, Dallas, TX, USA) and anti-myc (1:50; Proteintech, Rosemont, IL, USA (cat # 60003-2)) were used for hGBP-1. Anti-Drp1 (1:750; sc-101270) were from SCBT, Dallas, TX, USA. DAPI (4′,6-diamidino-2-phenylindole; 75 nM) was used for nuclear staining. The primary antibodies were detected by incubation with highly cross-absorbed Alexa 488-conjugated anti-rabbit (1:500), Alexa 488-conjugated anti-mouse (1:5000), Alexa 594-conjugated anti-rat (1:500), and Alexa 594-conjugated anti-mouse (1:500). Cells were washed with PBS and stained with 150 nM DAPI for 5 min at RT. Coverslips were mounted with Fluoromount-G (SouthernBotech, Birmingham, AL, USA). Epifluorescent images were captured using an EVOS FL inverted microscope by American Microscope Group (AMG) (Thermo Fisher Scientific, Carlsbad, CA, USA) with a 40X oil objective and GFP, Texas Rd, Cy5, and DAPI filters. Confocal images were collected using a TCS-SP 5 spectrophotometric multiphoton laser scanning confocal microscope (Leica Microsystems, Deer Park, IL, USA) collecting 0.2–1 μm optical sections. At least 2 independent experiments were performed for each of the localization studies. Representative examples are shown.

4.4. Mitochondrial Isolation

Mitochondria were isolated from GBM cells using the Mitochondria Isolation Kit for Cultured Cells (Thermo Scientific, Carlsbad, CA, USA), following the manufacturer's directions. Cells ($1.5–2 \times 10^7$) were grown in 150 mm dishes, scraped, and their pellets were frozen at −80 °C. The pellet from a single 150 mm dish was used for each mitochondrial isolation. Briefly, after cell lysis, the nuclei were removed by a low-speed centrifugation. The total cell lysate (TCL) aliquot was taken at that time. Further centrifugations separated the mitochondrial fraction from the cytosol. Alter lysis of the mitochondria, the protein levels of the TCL, cytosol, and mitochondrial fraction were determined and equal amounts of protein from each fraction were separated by SDS-PAGE and analyzed by western blot as described above. The subcellular fractionation of U251 ± GBP-1 cells and SNB75 cells was performed at least twice.

4.5. Generation of Amino-Terminal Myc-Tagged GBP-1 in pIRES-hygro2

The generation of pCMV2(NH) Flag-hGBP-1 was described previously [60]. Next, an amino terminal myc-epitope tag was added to pIRES2-eGFP. pIRES2-eGFP was digested with *BglII* and *EcoR1* and purified. The myc epitope was generated by the hybridization of two oligonucleotides: forward 5′-gatctatggaacagaaactgatcagcgaggaagatctgaatcgcggccgcc-3′ and reverse 5′-aattcgcggccgcgattcagatcttcctcgctgatcagtttctgttccata-3′. When the oligos are annealed, the 5- end has an overhang compatible with a *BglII* site and the 3′ end is compatible with an *EcoRI* site. Ligation of the double stranded oligonucleotide generated

c-myc pIRES2-eGFP. To generate c-myc hGBP-1 pIRES2-eGFP, c-my pIRES2-eGFP was digested to completion with *SmaI* and then partially digested with *NotI*. The appropriate fragment was gel purified and ligated with purified hGBP-1 cDNA liberated from pCMV/flag/NH GBP-1 by *SmaI/NotI* digestion. To generate c-myc hGBP-1 pIRES-hygro2, pIRES-hygro2 was cut to completion with *NheI/SmaI* and ligated to the insert released from c-myc hGBP-1-pIRES2-eGFP by *NheI/SmaI*. The construct was sequenced to assure fidelity.

4.6. Generation of U251 Cells Expressing Myc-Tagged hGBP-1

U251 cells were transfected with c-myc-hGBP1-pIRES-hygro2 (2 μg) or pIRES-hygro2 (2 μg). Transfection solutions were made at a lipid (μg) to plasmid (μL) ratio of 3:1 using FuGene 6 (Promega, Carlsbad, CA, USA) as the transfection reagent. Transfected U251 cells were selected in complete media with 50 μg/mL hygromycin. After 6 weeks of expansion from 12-well dishes to 10 cm dishes, twelve of the c-myc-hGBP1-pIRES-hygro2 transfected U251 colonies were analyzed by Western Blot for expression of hGBP-1. For further studies, the cells chosen were (control) A10 and (GBP-1 expressing cells) #4 and #7.

4.7. Mitochondrial Measurement

To measure mitochondrial length and width, cells were stained for TOMM40 to visualize the outer membranes of the mitochondria and imaged with a Leica TCS SP5 multiphoton confocal microscope at 0.2 μm optical sections. Following 3D reconstruction, the .lif files were opened in Leica's LASX program. The length and width of 10 mitochondria were measured from each of 20 randomly chosen cells for each cell type/condition. Individual mitochondria were first examined using the xyz format of the LASX program, which allows visualization through multiplanes. Once an individual mitochondrium was ready for analysis, the ruler icon was selected and the length and width of the mitochondrium was measured and expressed in μms. The data from two experiments were combined and analyzed using box and whisker plots from GraphPad Prism at 99% confidence interval. p values were determined by student's t-test.

4.8. Wound Healing Assay

SNB75 cells, U251 cells, and U251 cells containing myc-tagged GBP-1 were grown to confluence in flat bottom clear 96-well plates. Visual confluence was monitored for all seeded wells utilizing the IncuCyte S3 Live Cell Analysis System (Sartorius, Malvern, PA, USA). Prior to scratch, complete growth media was removed and replaced with serum free complete media for 4 h. After serum starvation, cells were "scratched" with a 96-well WoundMaker TM (Sartorius) and washed twice with sterile PBS to remove any suspended cells or debris caused by the scratch. Complete growth media was applied to all wells containing either DMSO or Mdivi-1 (Selleckchem Houston, TX, USA, Cat#S7162) resuspended in DMSO at 5 μM, 20 μM, or 50 μM. Mdivi-1 is the most frequently used Drp1 inhibitor, but it has some limitations [61]. Mdivi-1 can inhibit oxidative metabolism and modestly inhibit antioxidant activity [62,63]. Scratch closure was tracked every 2 h for 24 h via the IncuCyte S3 Live Cell Analysis System at 10× magnification. Wound width data analysis was generated for all wells utilizing the IncuCyte Scratch Wound analysis software module. Raw wound width data were exported and converted into wound % closure values for each individual sample with n = 5 per treatment group.

4.9. Statistics

Statistical analyses were carried out by two-tailed t-tests when two groups were analyzed. Statistically different groups are defined as * = p <0.05, ** = p < 0.01, and *** = p < 0.001.

5. Conclusions

The expression of GBP-1 and its association with mitochondria in GBM cells promotes the fission of mitochondria, resulting in shorter and wider mitochondria.

6. Note

While we were examining the consequence of GBP-1 localization to mitochondria in GBM cells, murine GBP-1 (mGBP-1) was shown to regulate the dysfunction of mitochondria and senescence in macrophages in vitro [64]. mGBP-1 is not confirmed to be the ortholog of human GBP-1. No evidence for a role in mitochondrial fission/fusion and cell migration/invasion was demonstrated in this study. In addition, during our study, GBP-2 was demonstrated to inhibit Drp-1-mediated fission in breast cancer cells, which inhibited cancer cell invasion [65].

Supplementary Materials: The following supporting information can be downloaded at: https://www.mdpi.com/article/10.3390/ijms252011236/s1.

Author Contributions: Conceptualization D.J.V. and A.L.N.-K.; methodology D.J.V., A.L.N.-K., M.P.M. and G.O.N.; validation S.M., M.P.M., A.L.N.-K. and D.J.V.; formal analysis D.J.V., M.P.M. and A.L.N.-K.; investigation R.C.K., G.O.N., M.P.M., S.M., J.S.J., A.L.N.-K. and D.J.V.; writing—original draft preparation D.J.V.; writing—review and editing, M.P.M., D.J.V., G.O.N., R.C.K., S.M., A.L.N.-K. and J.S.J.; visualization D.J.V., A.L.N.-K., M.P.M., R.C.K. and J.S.J.; supervision D.J.V. and A.L.N.-K., project administration D.J.V., funding acquisition D.J.V. and A.L.N.-K. All authors have read and agreed to the published version of the manuscript.

Funding: This work was supported by an Interdisciplinary Research Initiation Award and a Small Grant Support Award from the University of Toledo to D.J.V.

Institutional Review Board Statement: Not applicable.

Informed Consent Statement: Not applicable.

Data Availability Statement: Most of the data generated from this study are included in this article (and the Supplementary Data). The files containing the images used to measure the mitochondria can be made available upon request.

Acknowledgments: The authors thank Stephanie Angel for the generation of U251 cells containing myc-hGBP-1. The authors also thank William Maltese, Kathryn Eisenmann, Jean Overmeyer, and Krista Pettee for helpful discussions about glioblastoma and their culturing.

Conflicts of Interest: The authors declare no conflicts of interest.

References

1. Libermann, T.A.; Nusbaum, H.R.; Razon, N.; Kris, R.; Lax, I.; Soreq, H.; Whittle, N.; Waterfield, M.D.; Ullrich, A.; Schlessinger, J. Amplification and overexpression of the EGF receptor gene in primary human glioblastomas. *J. Cell Sci. Suppl.* **1985**, *3*, 161–172. [CrossRef] [PubMed]
2. Nishikawa, R.; Ji, X.D.; Harmon, R.C.; Lazar, C.S.; Gill, G.N.; Cavenee, W.K.; Huang, H.J. A mutant epidermal growth factor receptor common in human glioma confers enhanced tumorigenicity. *Proc. Natl. Acad. Sci. USA* **1994**, *91*, 7727–7731. [CrossRef] [PubMed]
3. Li, M.; Mukasa, A.; Inda, M.M.; Zhang, J.; Chin, L.; Cavenee, W.; Furnari, F. Guanylate binding protein 1 is a novel effector of EGFR-driven invasion in glioblastoma. *J. Exp. Med.* **2011**, *208*, 2657–2673. [CrossRef] [PubMed]
4. Lan, Q.; Wang, A.; Cheng, Y.; Mukasa, A.; Ma, J.; Hong, L.; Yu, S.; Sun, L.; Huang, Q.; Purow, B.; et al. Guanylate binding protein-1 mediates EGFRvIII and promotes glioblastoma growth in vivo but not in vitro. *Oncotarget* **2016**, *7*, 9680–9691. [CrossRef]
5. Johnson, H.; Del Rosario, A.M.; Bryson, B.D.; Schroeder, M.A.; Sarkaria, J.N.; White, F.M. Molecular characterization of EGFR and EGFRvIII signaling networks in human glioblastoma tumor xenografts. *Mol. Cell. Proteom. MCP* **2012**, *11*, 1724–1740. [CrossRef]
6. Ji, X.; Zhu, H.; Dai, X.; Xi, Y.; Sheng, Y.; Gao, C.; Liu, H.; Xue, Y.; Liu, J.; Shi, J.; et al. Overexpression of GBP1 predicts poor prognosis and promotes tumor growth in human glioblastoma multiforme. *Cancer Biomark.* **2019**, *25*, 275–290. [CrossRef]
7. Vestal, D.J.; Jeyaratnam, J.A. The Guanylate-Binding Proteins: Emerging insights into the biochemical properties and functions of this family of large interferon-induced guanosine triphosphatases. *J. Interferon Cytokine Res.* **2011**, *31*, 89–97. [CrossRef]
8. Tretina, K.; Park, E.S.; Maminska, A.; MacMicking, J.D. Interferon-induced guanylate-binding proteins: Guardians of host defense in health and disease. *J. Exp. Med.* **2019**, *216*, 482–500. [CrossRef]

9. Honkala, A.T.; Tailor, D.; Malhotra, S.V. Guanylate-Binding Protein 1: An Emerging Target in Inflammation and Cancer. *Front. Immunol.* **2019**, *10*, 3139. [CrossRef]
10. Kutsch, M.; Coers, J. Human guanylate binding proteins: Nanomachines orchestrating host defense. *FEBS J.* **2021**, *288*, 5826–5849. [CrossRef]
11. Praefcke, G.J.K. Regulation of innate immune functions by guanylate-binding proteins. *Int. J. Med. Microbiol.* **2018**, *308*, 237–245. [CrossRef] [PubMed]
12. Britzen-Laurent, N.; Bauer, M.; Berton, V.; Fischer, N.; Syguda, A.; Reipschläger, S.; Naschberger, E.; Herrmann, C.; Stürzl, M. Intracellular trafficking of guanylate-binding proteins is regulated by heterodimerization in a hierarchical manner. *PLoS ONE* **2010**, *5*, e14246. [CrossRef] [PubMed]
13. Praefcke, G.J.K.; McMahon, H.T. The dynamin superfamily: Universal membrane tubulation and fission molecules. *Nat. Rev. Mol. Cell Biol.* **2004**, *5*, 133–147. [CrossRef] [PubMed]
14. Prakash, B.; Praefcke, G.J.K.; Renault, L.; Wittinghofer, A.; Herrmann, C. Structure of human guanylate-binding protein 1 representing a unique class of GTP-binding proteins. *Nature* **2000**, *403*, 567–571. [CrossRef] [PubMed]
15. Prakash, B.; Renault, L.; Praefcke, G.J.K.; Herrmann, C.; Wittinghofer, A. Triphosphate structure of guanylate-binding protein 1 and implications for nucleotide binding and GTPase mechanism. *EMBO J.* **2000**, *19*, 4555–4564. [CrossRef]
16. Vopel, T.; Syguda, A.; Britzen-Laurent, N.; Kunzelmann, S.; Ludemann, M.B.; Dovengerds, C.; Sturzl, M.; Herrmann, C. Mechanism of GTPase-activity-induced self-assembly of human guanylate binding protein 1. *J. Mol. Biol.* **2010**, *400*, 63–70. [CrossRef]
17. Abdullah, N.; Srinivasan, B.; Modiano, N.; Cresswell, P.; Sau, A.K. Role of individual domains and indentification of internal gap in human Guanylate Binding Protein-1. *J. Mol. Biol.* **2009**, *368*, 690–703. [CrossRef]
18. Neun, R.; Richter, M.F.; Staeheli, P.; Schwemmle, M. GTPase properties of the interferon-induced human guanylate-binding protein 2. *FEBS Lett.* **1996**, *390*, 69–72. [CrossRef]
19. Schwemmle, M.; Staeheli, P. The interferon-induced 67-kDa guanylate-binding protein (hGBP1) is a GTPase that converts GTP to GMP. *J. Biol. Chem.* **1994**, *269*, 11299–11305. [CrossRef]
20. Praefcke, G.J.K.; Kloep, S.; Benscheid, U.; Lillie, H.; Prakash, B.; Herrmann, C. Identification of residues in the human guanylate-binding protein 1 critical for nucleotide binding and cooperative GTP hydrolysis. *J. Molec. Biol.* **2004**, *344*, 257–269. [CrossRef]
21. Cheng, Y.E.; Colonno, R.J.; Yin Fay, H. Interferon induction of fibroblast proteins with guanylate binding activity. *J. Biol. Chem.* **1983**, *258*, 7746–7750. [CrossRef] [PubMed]
22. Ghosh, A.; Praefcke, C.J.; Renault, L.; Wittinghofer, A.; Herrmann, C. How guanylate-binding proteins acheive assembly stimulated processive cleavage of GTP to GMP. *Nature* **2006**, *440*, 101–104. [CrossRef] [PubMed]
23. Syguda, A.; Bauer, M.; Benscheid, U.; Ostler, N.; Naschberger, E.; Ince, S.; Stürzl, M.; Herrmann, C. Tetramerization of human guanylate-binding protein 1 is mediated by coiled-coil formation of the C-terminal α-helices. *FEBS J.* **2012**, *279*, 2544–2554. [CrossRef] [PubMed]
24. Vöpel, T.; Kunzelmann, S.; Herrmann, C. Nucleotide dependent cysteine reactivity of hGBP1 uncovers a domain movement during GTP hydrolysis. *FEBS Lett.* **2009**, *583*, 1923–1927. [CrossRef]
25. Tripal, P.; Bauer, M.; Naschberger, E.; Mortinger, T.; Hohenadl, C.; Cornali, E.; Thurau, M.; Sturzl, M. Unique features of different members of the human Guanylate-Binding Protein family. *J. Interferon Cytokine Res.* **2007**, *27*, 44–52. [CrossRef]
26. Cheon, H.; Borden, E.C.; Stark, G.R. Interferons and their stimulated genes in the tumor microenvironment. *Semin. Oncol.* **2014**, *41*, 156–173. [CrossRef]
27. Santos, J.C.; Broz, P. Sensing of invading pathogens by GBPs: At the crossroads between cell-autonomous and innate immunity. *J. Leukoc. Biol.* **2018**, *104*, 729–735. [CrossRef]
28. Kim, B.-H.; Shenoy, A.R.; Kumar, P.; Bradfield, C.J.; MacMicking, J.D. IFN-inducible GTPases in host cell defense. *Cell Host Microbe* **2012**, *12*, 432–444. [CrossRef]
29. Guenzi, E.; Topolt, K.; Cornali, E.; Lubeseder-Martellato, C.; Jorg, A.; Matzen, K.; Zietz, C.; Kremmer, E.; Nappi, F.; Schwemmle, M.; et al. The helical domain of GBP-1 mediates the inhibition of endothelial cell proliferation by inflammatory cytokines. *EMBO J.* **2001**, *20*, 5568–5577. [CrossRef]
30. Guenzi, E.; Topolt, K.; Lubeseder-Martellato, C.; Jorg, A.; Naschberger, E.; Benelli, R.; Albini, A.; Sturzl, M. The guanylate binding protein-1 GTPase controls the invasive and angiogenic capabiliy of endothelial cells through inhibition of MMP-1 expression. *EMBO J.* **2003**, *22*, 3772–3782. [CrossRef]
31. Zhao, Y.; Wu, J.; Li, L.; Zhang, H.; Zhang, H.; Li, J.; Zhong, H.; Lei, T.; Jin, Y.; Xu, B.; et al. Guanylate-Binding Protein 1 as a Potential Predictor of Immunotherapy: A Pan-Cancer Analysis. *Front. Genet.* **2022**, *13*, 820135. [CrossRef] [PubMed]
32. Fukumoto, M.; Amanuma, T.; Kuwahara, Y.; Shimura, T.; Suzuki, M.; Mori, S.; Kumamoto, H.; Saito, Y.; Ohkubo, Y.; Duan, Z.; et al. Guanine nucleotide-binding protein 1 is one of the key molecules contributing to cancer cell radioresistance. *Cancer Sci.* **2014**, *105*, 1351–1359. [CrossRef] [PubMed]
33. Tipton, A.R.; Nyabuto, G.O.; Trendel, J.A.; Mazur, T.M.; Wilson, J.P.; Wadi, S.; Justinger, J.S.; Moore, G.L.; Nguyen, P.T.; Vestal, D.J. Guanylate-Binding Protein-1 protects ovarian cancer cell lines but not breast cancer cell lines from killing by paclitaxel. *Biochem. Biophys. Res. Commun.* **2016**, *478*, 1617–1623. [CrossRef] [PubMed]

34. Zhao, J.; Zhang, J.; Yu, M.; Xie, Y.; Huang, Y.; Wolff, D.W.; Abel, P.W.; Tu, Y. Mitochondrial dynamics regulates migration and invasion of breast cancer cells. *Oncogene* **2013**, *32*, 4814–4824. [CrossRef] [PubMed]
35. Schatz, G. The protein import system of mitochondria. *J. Biol. Chem.* **1996**, *271*, 31763–31766. [CrossRef]
36. Garrido, C.; Galluzzi, L.; Brunet, M.; Puig, P.E.; Didelot, C.; Kroemer, G. Mechanisms of cytochrome c release from mitochondria. *Cell Death Differ.* **2006**, *13*, 1423–1433. [CrossRef]
37. Xie, C.; Wang, F.Y.; Sang, Y.; Chen, B.; Huang, J.H.; He, F.J.; Li, H.; Zhu, Y.; Liu, X.; Zhuang, S.M.; et al. Mitochondrial Micropeptide STMP1 Enhances Mitochondrial Fission to Promote Tumor Metastasis. *Cancer Res.* **2022**, *82*, 2431–2443. [CrossRef]
38. Daumke, O.; Praefcke, G.J. Invited review: Mechanisms of GTP hydrolysis and conformational transitions in the dynamin superfamily. *Biopolymers* **2016**, *105*, 580–593. [CrossRef]
39. Ostler, N.; Britzen-Laurent, N.; Leible, A.; Naschberger, E.; Lochnit, G.; Ostler, M.; Forster, F.; Kunzelmann, P.; Ince, S.; Supper, V.; et al. Gamma interferon-induced Guanylate-Binding Protein 1 is a novel actin cytoskeleton remodeling factor. *Mol. Cell Biol.* **2014**, *34*, 196–209. [CrossRef]
40. Duan, Z.; Foster, R.; Brakora, K.A.; Yusuf, R.Z.; Seiden, M.V. GBP1 overexpression is associated with a paclitaxel resistance phenotype. *Cancer Chemother. Pharmacol.* **2005**, *57*, 25–33. [CrossRef]
41. Kalia, R.; Frost, A. Open and cut: Allosteric motion and membrane fission by dynamin superfamily proteins. *Mol. Biol. Cell* **2019**, *30*, 2097–2104. [CrossRef]
42. Duan, Z.; Lamendola, D.E.; Duan, Y.; Yusaf, R.; Seiden, M.V. Description of paclitaxel resistance-associated genes in ovarian and breast cancer cell lines. *Cancer Chemother. Pharmacol.* **2005**, *55*, 277–285. [CrossRef] [PubMed]
43. Bartolak-Suki, E.; Imsirovic, J.; Nishibori, Y.; Krishnan, R.; Suki, B. Regulation of mitochondrial structure and dynamics by the cytoskeleton and mechanical forces. *Int. J. Mol. Sci.* **2017**, *18*, 1812. [CrossRef] [PubMed]
44. Hatch, A.L.; Ji, W.-K.; Merrill, R.A.; Strack, S.; Higgs, H.N. Actin filaments as dynamic reservoirs for Drp1 recruitment. *Mol. Biol. Cell* **2016**, *27*, 3109–3121. [CrossRef] [PubMed]
45. Moore, A.S.; Wond, Y.C.; Simpson, C.L.; Holzbaur, E.L.F. Dynamic actin cycling through mitochondrial subpopulations locally regulates the fission-fusion balance within mitochondrial networks. *Nat. Commun.* **2015**, *7*, 12886. [CrossRef] [PubMed]
46. Ramachandran, R.; Schmid, S.L. The dynamin superfamily. *Curr. Biol.* **2018**, *28*, R411–R416. [CrossRef]
47. Ramachandran, R. Mitochondrial dynamics: The dynamin superfamily and execution by collusion. *Semin. Cell Dev. Biol.* **2018**, *76*, 201–212. [CrossRef]
48. Kraus, F.; Roy, K.; Pucadyil, T.J.; Ryan, M.T. Function and regulation of the divisome for mitochondrial fission. *Nature* **2021**, *590*, 57–66. [CrossRef]
49. Kraus, F.; Ryan, M.T. The constriction and scission machineries involved in mitochondrial fission. *J. Cell Sci.* **2017**, *130*, 2953–2960. [CrossRef]
50. Jimah, J.R.; Hinshaw, J.E. Structural insights into the mechanism of dynamin superfamily proteins. *Trends Cell Biol.* **2019**, *29*, 257–273. [CrossRef]
51. Srinivasan, S.; Guha, M.; Kashina, A.; Avadhani, N.G. Mitochondrial dysfunction and mitochondrial dynamics-The cancer connection. *Biochim. Biophys. Acta Bioenerg.* **2017**, *1858*, 602–614. [CrossRef] [PubMed]
52. Pendin, D.; Filadi, R.; Pizzo, P. The Concerted Action of Mitochondrial Dynamics and Positioning: New Characters in Cancer Onset and Progression. *Front. Oncol.* **2017**, *7*, 102. [CrossRef] [PubMed]
53. Caino, M.C.; Altierri, D.C. Cancer cell exploit adaptive mitochondrial dynamics to increase tumor cell invasion. *Cell Cycle* **2015**, *14*, 3242–3247. [CrossRef] [PubMed]
54. Amiri, M.; Hollenbeck, P.J. Mitochondrial biogenesis in the axons of vertebrate peripheral neurons. *Dev Neurobiol* **2008**, *68*, 1348–1361. [CrossRef] [PubMed]
55. Sprenger, H.G.; Langer, T. The Good and the Bad of Mitochondrial Breakups. *Trends Cell Biol.* **2019**, *29*, 888–900. [CrossRef]
56. Jo, Y.; Cho, H.M.; Sun, W.; Ryu, J.R. Localization of dynamin-related protein 1 and its potential role in lamellipodia formation. *Histochem. Cell Biol.* **2017**, *148*, 13–20. [CrossRef]
57. Huang, L.; Luan, T.; Chen, Y.; Bao, X.; Huang, Y.; Fu, S.; Wang, H.; Wang, J. LASS2 regulates invasion and chemoresistance via ERK/Drp1 modulated mitochondrial dynamics in bladder cancer cells. *J. Cancer* **2018**, *9*, 1017–1024. [CrossRef]
58. Lima, A.R.; Santos, L.; Correia, M.; Sobrinho-Simoes, M.; Melo, M.; Maximo, V. Dynamin-Related Protein 1 at the Crossroads of Cancer. *Genes* **2018**, 115. [CrossRef]
59. Pagliuso, A.; Cossart, P.; Stavru, F. The ever-growing complexity of the mitochondrial fission machinery. *Cell. Mol. Life Sci. CMLS* **2018**, *75*, 355–374. [CrossRef]
60. Wadi, S.; Tipton, A.R.; Trendel, J.A.; Khuder, S.A.; Vestal, D.J. hGBP-1 Expression Predicts Shorter Progression-Free Survival in Ovarian Cancers, While Contributing to Paclitaxel Resistance. *J. Cancer Ther.* **2016**, *7*, 994–1007. [CrossRef]
61. Smith, G.; Gallo, G. To mdivi-1 or not to mdivi-1: Is that the question? *Dev. Neurobiol.* **2017**, *77*, 1260–1268. [CrossRef] [PubMed]
62. Bordt, E.A.; Clerc, P.; Roelofs, B.A.; Saladino, A.J.; Tretter, L.; Adam-Vizi, V.; Cherok, E.; Khalil, A.; Yadava, N.; Ge, S.X.; et al. The Putative Drp1 Inhibitor mdivi-1 Is a Reversible Mitochondrial Complex I Inhibitor that Modulates Reactive Oxygen Species. *Dev. Cell* **2017**, *40*, 583–594. [CrossRef] [PubMed]
63. Dai, W.; Wang, G.; Chwa, J.; Oh, M.E.; Abeywardana, T.; Yang, Y.; Wang, Q.A.; Jiang, L. Mitochondrial division inhibitor (mdivi-1) decreases oxidative metabolism in cancer. *Br. J. Cancer* **2020**, *122*, 1288–1297. [CrossRef] [PubMed]

64. Qiu, X.; Guo, H.; Yang, J.; Ji, Y.; WU, C.-S.; Chen, X. Down-regulation of guanylate binding protein 1 causes mitochondrial dysfunction and cellular senescence in macrophages. *Sci. Rep.* **2018**, *8*, 1679. [CrossRef]
65. Zhang, J.; Zhang, Y.; Wu, W.; Wang, F.; Liu, X.; Shui, G.; Nie, C. Guanylate-binding protein 2 regulates Drp1-mediated mitochondrial fission to suppress breast cancer cell invasion. *Cell Death Dis.* **2017**, *8*, e3151, Correction in *Cell Death Dis.* **2018**, *9*, 1127. [CrossRef]